

Dark-line atomic resonances in a submicron-thin Rb vapor layer

A. Sargsyan,^{1,2} D. Sarkisyan,^{1,*} and A. Papoyan¹

¹*Institute for Physical Research, NAS of Armenia, Ashtarak-2 378410, Armenia*

²*Yerevan State University, A. Manoogian Street 1, Yerevan 375049, Armenia*

(Received 28 October 2005; published 2 March 2006)

We report an experimental investigation of the effect of electromagnetically induced transparency (EIT) using bichromatic laser radiation and an extremely thin cell filled with pure Rb with smoothly controllable thickness L of the atomic vapor layer in the range $\sim 780\text{--}1600$ nm, for which L is comparable to the laser wavelength λ resonant with the D_2 line (780 nm). It is revealed that the transmission spectrum of the probe laser contains two sub-Doppler peaks that have different linewidths. The narrow peak corresponds to EIT, whereas the broader one results from velocity-selective optical pumping (VSOP) and repumping processes. It is demonstrated that in the case of nonzero detuning of the coupling laser, the EIT resonance and VSOP are shifted with respect to each other on the frequency scale, which makes it possible to observe a competition between the two effects (this is not possible to realize in an ordinary cell). Also, the Dicke-type coherent narrowing effect depending on the ratio L/λ influences the absorption spectrum of the probe laser. Formation of an EIT resonance is substantially favored for the atoms with slow normal velocity, caused by their longer interaction time with the bichromatic laser field. As a result of the predominant contribution of these atoms, the observed linewidth of the EIT resonance is only ~ 9 MHz, which is more than ten times narrower than the inverse window-to-window flight time. In an external magnetic field, three and five EIT resonances have been observed for the vapor thickness of $L=2\lambda$, on ^{87}Rb and ^{85}Rb , respectively.

DOI: [10.1103/PhysRevA.73.033803](https://doi.org/10.1103/PhysRevA.73.033803)

PACS number(s): 42.50.Gy, 42.62.Fi, 42.50.Md

In pioneering experimental work [1] it has been experimentally demonstrated that a resonant laser-atom interaction in a thin film of alkali-metal vapor with thickness $L=10\text{--}1000$ μm provides a novel method for sub-Doppler spectroscopy. Recently, with the help of an extremely thin cell (ETC) filled with alkali metal it was demonstrated that there is clearly a length of $L=\lambda/2$ (λ is the laser resonant wavelength) for which the absorption and fluorescence spectra are approximately ten times narrower than the Doppler width [2–4]. For $L=n\lambda$ (n is integer), sub-Doppler peaks of reduced absorption, centered on the hyperfine atomic transitions, appear in the transmission spectra [1,4,5]. Note that since a single beam is used, there are no crossover resonances. This is important when there are many overlapped spectral lines as is the case for the D_2 line of ^{85}Rb , $F_g=2 \rightarrow F_e=1,2,3$ transitions [5], and this technique has been used in this work for frequency reference spectra formation. However, the linewidth of these peaks is principally limited to the atomic natural linewidth ($\gamma_N \sim 6$ MHz).

The recent interest in the electromagnetically induced transparency (EIT) phenomenon is caused by the possibility of forming narrow resonances, as well as by a number of important applications [6–17]. EIT resonances can occur in a Λ system with two long-lived ground states and one excited state coupled by two laser fields. In order to achieve narrow EIT resonance, two lasers have to be coherently coupled [9–11], and for this purpose several modulation techniques can be implemented [9]. However, there are some situations, for example as in the case of EIT in indium vapor [15], when

the frequency separation of the two ground states is very large and thus the only possibility is to use two different lasers.

The linewidth of the EIT resonance in the case of low laser intensity is $\gamma_{EIT} \approx 2\Gamma_{21} + \Omega^2/\gamma_N$ [16], where Γ_{21} is the relaxation rate between the ground hyperfine levels, with Ω being the Rabi frequency. For the case of an ETC, the value of Γ_{21} is highly affected by atom-wall (window) collisions. It is known that a unique collision with the dielectric surface of an uncoated vapor cell is sufficient to thermalize the ground hyperfine levels, with depolarization probability 0.5–1 [18]. This assumption was used for development of a theoretical model [19] describing experimental results of the absorption and fluorescence spectra when the thickness of the atomic vapor column is of order of λ [4]. The model, which implies complete loss of optical excitation and equalization of population of the ground levels $|1\rangle$ and $|2\rangle$ for a single collision, was in good agreement with the experiment. The same assumption has been made in [17], in order to describe the EIT process in a thin cell. Note that in order to preserve the atomic coherence in wall collisions and to detect ultranarrow linewidths with the help of coherent processes like EIT, nonlinear magneto-optical rotation, and others, paraffin-coated walls are used [20]. As the size of the vapor cell is reduced, the lifetime of the ground-state coherence becomes shorter because of collisions of the atoms with the cell windows: $\Gamma_{21}=(2\pi t)^{-1}$, where $t=L/u$ (L is the distance between the windows, and u is the most probable thermal velocity). Also, the EIT resonance contrast (defined as the ratio of the EIT depth to the height of the shoulders of the EIT window) strongly depends on Γ_{21} . Hence, in the case of $L \sim 1$ μm ($2\Gamma_{21} > 100$ MHz), one could expect that the EIT effect will vanish. In order to prevent atom-window collisions for the

*Corresponding author. Fax: 00374-232-31172. Electronic address: david@ipr.sci.am

case of submillimeter-thin cells, buffer gas has been successfully used in [14]. Nevertheless, in [17] it was predicted that even in the case of pure atomic vapor, narrow EIT resonance can be observed for a cell with $L \sim 10 \mu\text{m}$. The explanation is that the contribution of atoms with slow normal velocity is enhanced thanks to their longer interaction time with laser fields. Consequently, the atoms flying nearly parallel to the windows yield a stronger contribution to the EIT resonance. The observation of Hanle resonance in Cs vapor for a thickness of the vapor column $L = \lambda = 852 \text{ nm}$ was reported in [21].

Here we present the results of an EIT study in an ETC filled with pure Rb and with smoothly variable thickness L of atomic vapor in the range $\sim 780\text{--}1600 \text{ nm}$. Note that L is 100 times smaller than that previously reported with bichromatic laser use ($L \sim 0.1 \text{ mm}$) [14]. In [22] the EIT effect has been studied in the selective reflection (SR) process on the Rb D_1 line in a several-centimeter-long cell, and though for this case the vapor column is limited from one side by the cell window, the second boundary is diffuse; thus the thickness is not well determined: as was demonstrated in [3,23], there is a dramatic difference for the SR spectra obtained in an ordinary cell and in a thin vapor layer.

The ETC design is similar to that described in [2] but has several distinctions. The windows, 30 mm in diameter and 3 mm thick, were made from sapphire, which is chemically resistant to the hot vapors of alkali metals, as well as In [15]. In order to minimize the birefringence effect, the sapphire plates were cut across the c axis. To form a required 3000-nm-thick wedged gap, an Al_2O_3 strip, 10 mm long and 1 mm wide, was deposited on the surface of one window in its lower part. The wedge-shaped (vertically) thickness L of the gap was determined by an interferometric method [3], and was found to range from 350 to 2800 nm. The ETC operated with an oven made from nonmagnetic materials.

As is shown in Fig. 1(a), our Λ -type system is formed on the atomic D_2 line of ^{85}Rb (^{87}Rb). The ground-state hyperfine levels $F_g=2$ and $F_g=3$ ($F_g=1$ and $F_g=2$), spaced by 3036 MHz (6835 MHz), serve as the two lower states, and the excited state $5P_{3/2}$ serves as the common upper level. The experimental arrangement is sketched in Fig. 1(b). The beams ($\varnothing 3 \text{ mm}$) of two single-frequency diode lasers with $\lambda \approx 780 \text{ nm}$ (the spectral width is $\sim 5 \text{ MHz}$) are well superposed and focused by an $F=35 \text{ cm}$ lens into the ETC at nearly normal incidence. The first Glan prism ensures a high degree of linear polarization of the laser radiation (the beams have parallel linear polarization), while the second Glan prism allows one to smoothly vary the intensity of the transmitted radiation. The ETC was placed in three pairs of mutually perpendicular Helmholtz coils (1) providing the possibility to cancel the laboratory magnetic field as well as to apply a homogeneous magnetic field. The optical radiations were recorded by the photodiodes (2) followed by operation amplifiers and recorded by a two-channel digital storage oscilloscope Tektronix TDS 3032B. The intensities of the coupling and probe lasers were $\approx 0.1 \text{ W/cm}^2$ and $15\text{--}50 \text{ mW/cm}^2$, respectively.

In order to clarify the expected peculiarities of the EIT resonance, presented in Fig. 2 is the transmission spectrum of ETC ($^{85}\text{Rb } F_g=3 \rightarrow F_e=2,3,4$) when only the probe laser

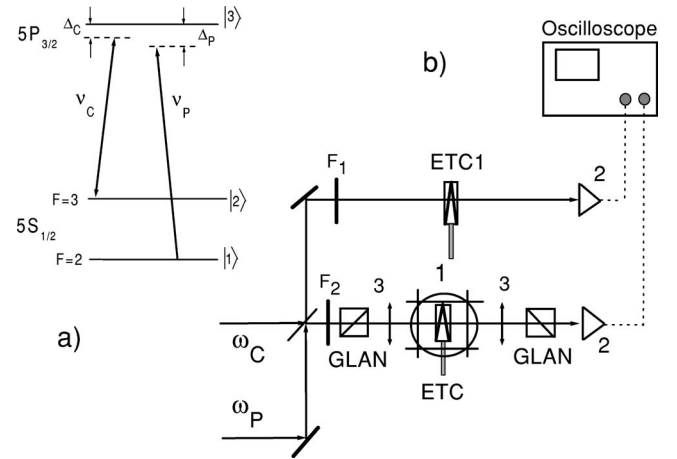


FIG. 1. (a) Sketch of the relevant energy levels of Rb D_2 transitions and Λ -type three-level scheme; Δ_C and Δ_P are the detunings of the coupling and probe lasers, respectively. (b) Experimental setup (schematic): ω_C , coupling laser; ω_P , probe laser; ETC1 and ETC, reference and main extremely thin cells, respectively; F_1 , F_2 , attenuators; 1, Helmholtz coils; 2, light detectors; 3, lenses; $F = 35 \text{ cm}$.

is used. The thicknesses L is varied in the range of $\lambda/2\text{--}2\lambda$ (390–1560 nm), and the laser intensity is $\sim 0.1 \text{ mW/cm}^2$ [Fig. 2(a)]. The effect of the so-called Dicke-type spectral coherent narrowing regime (DCNR) [3,4] is well observable: at $L = \lambda/2$ the linewidth is minimal, at $L = 3\lambda/2$ the narrowing is observed on a wide base, whereas the maximal values of the linewidth are observed at $L = \lambda$ and 2λ . Similar spectra are presented in Fig. 2(b) for the laser intensity $\sim 40 \text{ mW/cm}^2$. The peaks of DCNR in transmission with strong modification of spectra (compared with the low-intensity case) are still observable at the thicknesses $L = \lambda/2$ and $3\lambda/2$; meanwhile sub-Doppler saturation or optical pumping peaks are clearly seen in transmission at $L = \lambda$ and 2λ . Note that at $L = 3\lambda/2$ the coherent narrowing is formed in the wide dip of reduced absorption due to velocity-selective optical pumping or saturation effects. Similar spectra are observed on scanning the laser frequency

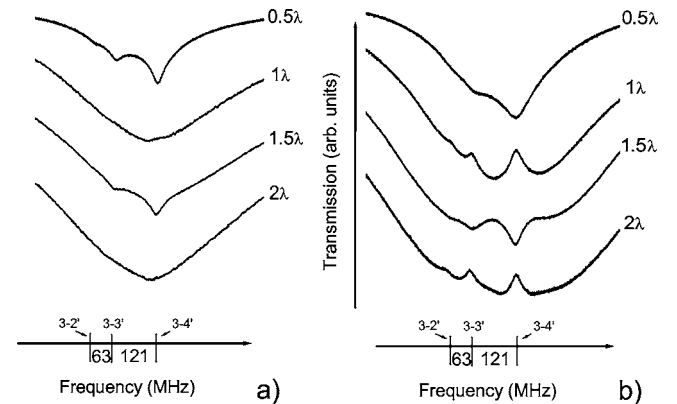


FIG. 2. Transmission spectra of Rb vapor layer with smoothly controllable thickness in the range $L = 390\text{--}1560 \text{ nm}$; $^{85}\text{Rb } F_g=3 \rightarrow F_e=2,3,4$ transitions, laser intensity (a) ~ 0.1 and (b) 40 mW/cm^2 .

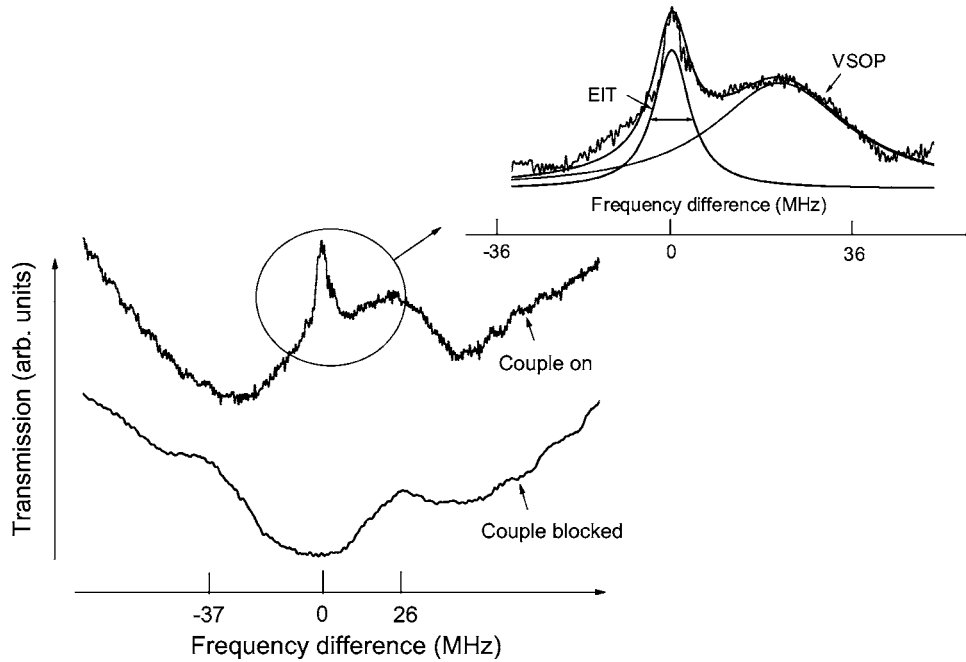


FIG. 3. Probe laser transmission spectrum, $L=2\lambda$ (1560 nm), coupling laser is red detuned by 26 MHz from the $F_g=3 \rightarrow F_e=3$ transition, $I_C \approx 0.1$ W/cm², probe is scanned across $F_g=2 \rightarrow F_e=1, 2, 3$ transitions, $I_P \approx 15$ mW/cm², $T_W \approx 170$ °C, and $T_{SA} \approx 150$ °C. The EIT resonance is seen in the upper curve together with VSOP. The inset shows the results of fitting by a Lorentzian line; FWHM widths of the EIT resonance and VSOP are ≈ 9 and ≈ 33 MHz, respectively. Note that in the presence of the coupling laser, the probe absorption is enhanced on $F_g=2 \rightarrow F_e=2$ due to optical repumping (the coupling laser removes atoms from $F_g=3$ to 2), and instead of the peak there is a dip, while on the lower curve (the case when the coupling laser is blocked, shifted vertically for convenience) the peak of reduced absorption due to VSOP is well seen.

across the $^{85}\text{Rb } F_g=2 \rightarrow F_e=1, 2, 3$ and $^{87}\text{Rb } F_g=1 \rightarrow F_e=0, 1, 2$ transitions (the transmission spectra when L varies in the range of $\lambda/2 - 7\lambda/2$ were presented in [5]).

Let us describe briefly the technique of frequency reference spectra formation with the ETC1: as is mentioned above, the peaks of reduced absorption, which are centered on the hyperfine atomic transitions, occur in the transmission spectra (incident intensity is a few mW/cm²) at near-normal incidence when $L=\lambda$ [1,4]. The operation temperature of ETC1 was $T_W \sim 130$ °C at the window, and $T_{SA} \sim 100$ °C at the side-arm.

As was demonstrated in [3,4], and also shown in Fig. 2, the main peculiarities of the probe laser transmission line shape are observable at $L=(2n+1)\lambda/2$ and $L=n\lambda$. For this reason, we present below the EIT results for the thicknesses $L=2\lambda$, $3\lambda/2$, and λ . No additional features were revealed for intermediate L values. Figure 3 shows the transmission spectrum when the vapor thickness is $L=2\lambda$ (1.56 μm), the coupling laser ($I_C \sim 0.1$ W/cm²) is red detuned by 26 MHz from the $^{85}\text{Rb } F_g=3 \rightarrow F_e=3$ transition, and the probe ($I_P \sim 15$ mW/cm²) is scanned across $^{85}\text{Rb } F_g=2 \rightarrow F_e=1, 2, 3$ transitions ($T_W \sim 170$ °C, $T_{SA} \sim 150$ °C, and taking into account the isotopic abundance of natural Rb, $N \sim 6 \times 10^{13}$ cm⁻³). As was predicted in [17], under the condition of exact resonance of the coupling laser with the corresponding atomic transition, the transmission spectrum of the probe contains the EIT resonance peak, together with the velocity-selective optical pumping (VSOP) peak (or dip for the absorption spectrum), which are superimposed on the fre-

quency scale, while in the case of nonzero detuning, these two peaks (dips) are shifted with respect to each other, which makes it possible to observe a competition between the two effects. In the upper curve of Fig. 3 the EIT resonance is seen together with the VSOP peak. The inset presents the results of Lorentzian fitting, which gives the full width at half maximum (FWHM) of the EIT resonance of ≈ 9 MHz, while the linewidth of the VSOP peak is ≈ 33 MHz (note that $2\Gamma_{21} \sim 63$ MHz for the atoms with the most probable thermal velocity ~ 310 m/s at $T_W \sim 170$ °C). Note that the coupling laser affects the probe absorption spectrum also outside the coherent population trapping frequency region, since it causes velocity-selective optical repumping of ground-state hyperfine levels, which were partly depleted by the probe laser. The detailed study of entire absorption spectra inside the Doppler profile will be presented elsewhere [24].

In Fig. 4 shown is the transmission spectrum when $L=1.5\lambda$ (1.17 μm). All parameters are the same as in Fig. 3, except that the coupling laser is resonant with $F_g=3 \rightarrow F_e=3$. In the upper curve, the EIT resonance is seen together with VSOP and Dicke revival peaks. The inset presents the results of fitting: the linewidth of the EIT resonance is ≈ 9 MHz, and the VSOP linewidth is ≈ 35 MHz ($2\Gamma_{21} \sim 84$ MHz). The lower curve is the case when the coupling laser is blocked, and the revival of the Dicke-narrowing effect is well seen.

In Fig. 5 is shown the transmission spectrum when $L=\lambda$ (780 nm), the coupling laser is blue detuned by 20 MHz from the $^{87}\text{Rb } F_g=2 \rightarrow F_e=2$ transition, while the probe is scanned across $^{87}\text{Rb } F_g=1 \rightarrow F_e=0, 1, 2$ transitions (for other

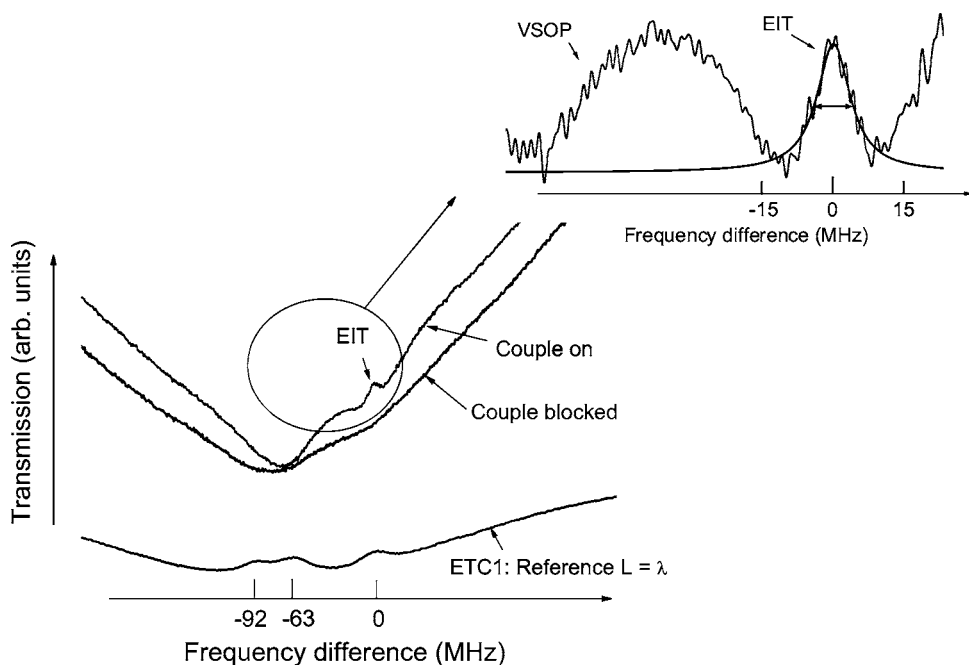


FIG. 4. Probe laser transmission spectrum, $L=1.5\lambda$ (1170 nm). All parameters are the same as in Fig. 3, except the coupling laser is resonant with $F_g=3 \rightarrow F_e=3$ transition. In the top curve the EIT resonance is seen together with VSOP and Dicke revival peak. Inset shows the results of fitting: the EIT resonance linewidth is ≈ 9 MHz, VSOP linewidth is ≈ 35 MHz. The middle curve shows the case when the coupling laser is blocked, and revival of Dicke-narrowing effect is well seen. The bottom curve is the transmission spectrum of the ETC1.

parameters, see the figure caption). In the upper curve the EIT resonance and VSOP peak are still clearly visible. The inset presents results of the fitting: the linewidth of the EIT is ~ 9 MHz, the VSOP linewidth is ≈ 32 MHz ($2\Gamma_{21} \sim 130$ MHz). The lower curve is the transmission of the reference ETC1. Note that decreasing of L from 2λ to λ does not cause broadening of the EIT resonance; only some reduction of contrast is observable. The latter means that merely slow atoms contribute to the EIT resonance formation.

The presented experimental results are in qualitative agreement with the theoretical model developed in [17]. In particular, the following predictions of [17] have been justified: (i) due to atomic velocity selectivity, it is possible to observe sub-Doppler EIT resonances in an uncoated buffer-gas-free ETC; (ii) the linewidth of EIT resonance is several times narrower than that of the VSOP; (iii) unlike the case of

ordinary cells, for a nonzero detuning of a coupling laser from an atomic transition, the EIT and VSOP resonances are frequency shifted from each other, and can be easily distinguished. Nevertheless, the quantitative comparison shows some discrepancies, which can be attributed to the somewhat simplified approach accepted in [17]. Thus, the model does not involve the contribution of a backward beam reflected by a rear window of the ETC, which is essential for the case of $L \sim \lambda$. Furthermore, the ground-state coherence in a real atom can be affected by the hyperfine structure of the upper state [25], which was also omitted in the model. We believe relevant modification of the model is required for better agreement. As to the EIT resonance linewidth, we consider three main physical reasons, which have influence on it: (i) the lasers are not coherently coupled [7]; (ii) the laser intensities are relatively high; (iii) the thickness of the ETC is

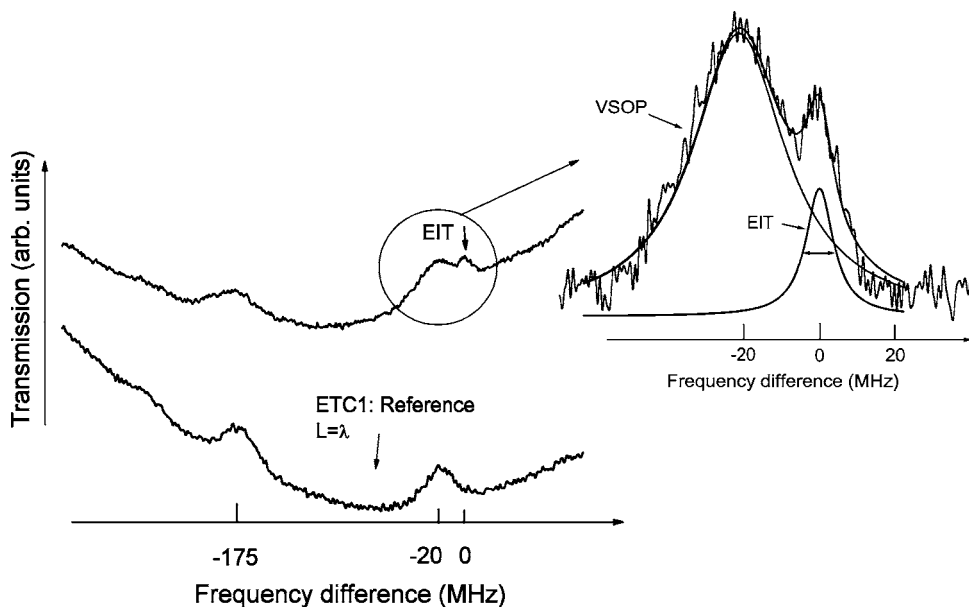


FIG. 5. Probe laser transmission spectrum for $L=\lambda$ (780 nm), coupling laser is blue detuned by 20 MHz from the $^{87}\text{Rb} F_g=2 \rightarrow F_e=2$ transition, $I_C \sim 0.1$ W/cm 2 , the probe laser is scanned across $F_g=1 \rightarrow F_e=0, 1, 2$ transitions, $I_P \sim 45$ mW/cm 2 , $T_W \sim 180$ $^\circ\text{C}$, $T_{SA} \sim 165$ $^\circ\text{C}$, and $N \sim 5 \times 10^{13}$ cm $^{-3}$. In the upper curve one can see the EIT resonance and VSOP peak. The inset presents results of the fitting: EIT resonance linewidth is ≈ 9 MHz; VSOP linewidth is ≈ 32 MHz. The lower curve is the transmission spectrum of the ETC1 (here the probe intensity is only ~ 5 mW/cm 2 , and the peaks are narrower).

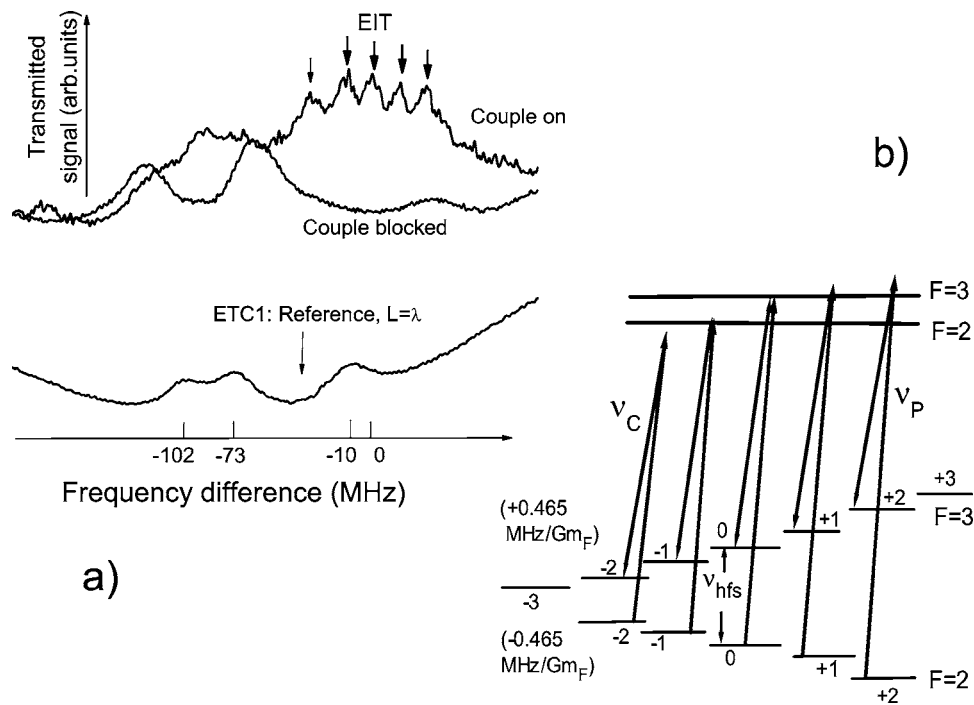


FIG. 6. (a) Upper curve is the transmission spectrum for Faraday-type configuration (see text); coupling beam is on. Longitudinal magnetic field is $B=15$ G, $L=2\lambda$; coupling laser is blue detuned by 10 MHz from the $^{85}\text{Rb } F_g=3 \rightarrow F_e=3$ transition; the probe laser is scanned across $F_g=2 \rightarrow F_e=1, 2, 3$; other parameters are the same as in Fig. 3. Five well-resolved ~ 9 MHz wide EIT resonances are clearly seen with the splitting value of ≈ 14 MHz. Zero-difference frequency corresponds to $\nu_P - \nu_C = 3036$ MHz. The gray curve corresponds to the case of blocked coupling beam, and lower curve is the transmission spectrum of the reference ETC1. Note that the maxima of the probe transmission are shifted with respect to the reference peaks. This is caused by reduction of the number of slow atoms on the initial ground level because of VSOP, while these atoms provide the main contribution into Faraday signal in the case of ETC [28]. (b) Hyperfine Zeeman energy level diagram of atomic ^{85}Rb (not to scale); $\nu_{hfs}=3036$ MHz. Zeeman splitting of the excited states is omitted, following [26], for simplicity. The sublevel linear Zeeman shift is $+0.465$ MHz/G $\times m_F$ and -0.465 MHz/G $\times m_F$ for the ground level $F=3$ and 2, respectively [29].

small. The contributions from each of these factors can be evaluated using the modified model to be developed.

The narrow width of the EIT resonance allowed us to examine its splitting in moderate magnetic field because of the Zeeman shift of the magnetic sublevels of the hyperfine states. This study is important to prove that the narrow resonance we observe is indeed associated with EIT, but not a VSOP-type process: the EIT resonance should split in the magnetic field into three and five resonances for ^{87}Rb and ^{85}Rb , respectively (see below). Observation of these resonances would be another convincing support for the EIT nature of the recorded peaks. To study this effect, a longitudinal magnetic field $B=15$ G was applied, and the angle of the second Glan prism [Fig. 1(b)] was adjusted to achieve maximum signal contrast [12]. Figure 6(a) shows the transmitted signal in this Faraday-type configuration¹ for the case of $L=2\lambda$. The coupling laser is blue detuned by 10 MHz from the $^{85}\text{Rb } F_g=3 \rightarrow F_e=3$ transition. The probe is scanned across $F_g=2 \rightarrow F_e=1, 2, 3$ transitions (for other parameters, see the figure caption). As is seen, five well-resolved EIT resonances (~ 9 MHz wide) are observable [as is shown in Fig. 6(b), five Λ systems based on the Zeeman sublevels are created in

this case]. The splitting value is 0.93 MHz/G $\times 15$ G ≈ 14 MHz. Note that the exact splitting for large B fields is given by the Rabi-Breit formula [26].

Similar spectra have been recorded also for the Λ system of ^{87}Rb [see Fig. 7(a)]. Here the coupling laser is blue detuned by 18 MHz from the $^{87}\text{Rb } F_g=2 \rightarrow F_e=2$; the probe is scanned across the $F_g=1 \rightarrow F_e=0, 1, 2$ transitions (for other parameters, see the figure caption). One can see three well-resolved EIT resonances of ~ 10 MHz linewidth [as shown in Fig. 7(b), in this case three Λ -systems are formed]. The frequency difference between the EIT resonances is 1.4 MHz/G $\times 15$ G ≈ 21 MHz. The substructure of the probe signal spectrum with no coupling beam [as is also the case in Fig. 6(a)] is caused by VSOP.

Let us now compare our results with the peculiarities of resonance formation in an ETC observed in other relevant works. In [27] it was shown that in the case of a two-photon absorption, when the sum of the exciting frequencies $\omega_1 + \omega_2$ is nearly resonant to the Cs $6S_{1/2}-6D_{5/2}$ transition, there is also clearly a length of $L=\Lambda/2$ with $\Lambda=2\pi/|\vec{k}_1+\vec{k}_2|$, where \vec{k}_1 and \vec{k}_2 are the wave vectors, for which the spectral width of the transmission line shape is minimal (several times narrower than a two-photon Doppler width). This effect is a two-photon analog of the DCNR observed in a one-photon transition for $L=\lambda/2$ [3,4]. In particular, when $\omega_1 \approx \omega_2$ and the radiations are collinear, the length of DCNR is

¹The results on conventional Faraday rotation studies in an ETC have been reported recently in [28].

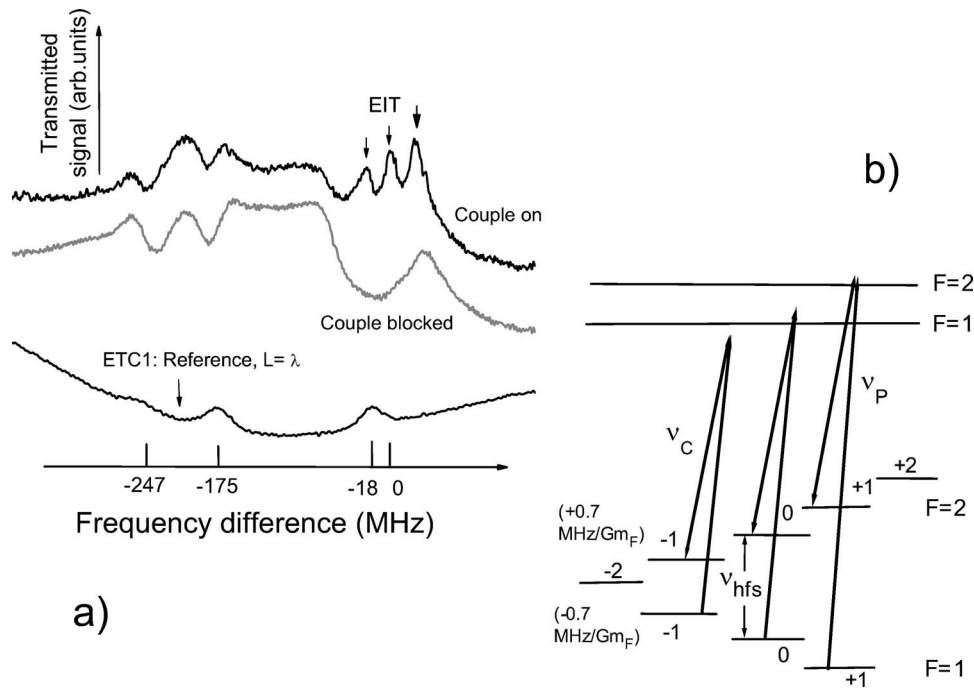


FIG. 7. (a) Upper curve is the transmission spectrum for Faraday-type configuration (see text); coupling beam is on. Longitudinal magnetic field $B=15$ G, $L=2\lambda$, the coupling laser is blue detuned by 18 MHz from the $^{87}\text{Rb } F_g=2 \rightarrow F_e=2$ transition; the probe laser is scanned across the $F_g=1 \rightarrow F_e=0,1,2$ transitions; other parameters are the same as in Fig. 5. Zero difference frequency corresponds to $\nu_P - \nu_C = 6835$ MHz. Three well-resolved EIT resonances (linewidth ≈ 10 MHz) are clearly seen, with the frequency separation of ≈ 21 MHz. The gray curve shows the probe Faraday-type transmission spectrum without coupling beam (shifted vertically for convenience). The substructure of this spectrum is caused by VSOP. (b) Hyperfine Zeeman energy level diagram of ^{87}Rb , $\nu_{hfs} = 6835$ MHz.

$L = \Lambda/2 = \lambda/4$. The main difference of one- and two-photon DCNR from an EIT resonance is that the latter is much narrower due to the different coherent nature (~ 9 MHz for $L = \lambda$, as opposed to 60–70 MHz for a one-photon DCNR at $L = \lambda/2$, and ~ 300 MHz for a two-photon DCNR at $L \sim 315$ nm). Furthermore, in contrast to one-photon DCNR, it is possible to vary the frequency of EIT resonance. Finally, the VSOP peaks observed in a one-photon transmission spectra for $L = \lambda$ and over 1 mW/cm^2 laser intensity are nearly twice broader than the EIT peaks, and are exactly centered (fixed) on the atomic transitions.

Coherent population trapping (CPT) resonance in a Λ system has been observed for $L = \lambda$ in [21] using the Hanle configuration: the resonance is obtained by scanning the magnetic field at a fixed laser frequency, and the width of the resonance is measured in magnetic field units. Conversion into the frequency domain shows that the linewidth of the CPT resonance is several tens of megahertz, which is much larger than the EIT resonance linewidth obtained in the present work. It should be noted that in [21], the ground levels are the Zeeman sublevels of the same hyperfine

ground state, while in our case the ground levels are two different hyperfine states.

To summarize, the effect of EIT has been studied with the help of an ETC with controllable thickness of vapor layer, in the range $\sim 780\text{--}1600$ nm. It is demonstrated that the transmission spectrum of the probe laser contains the EIT resonance, along with a several times broader VSOP peak. Note that the ETC-based magnetometer scheme proposed in [29], which allows for a submicrometer spatial resolution, can be improved by exploiting the EIT resonance. One can expect that the use of coherently coupled lasers will result in a narrow EIT linewidth and higher contrast, which could allow one to observe the ETC resonance below $L = 800$ nm, too. The case of particular interest is $L < 200$ nm, where narrow EIT resonances will be helpful for studies of atom-surface van der Waals interaction [30].

The authors are grateful to A. Sarkisyan for his valuable participation in fabrication of the ETC as well as to Yu. Malakyan, D. Bloch, and Y. Pashayan-Leroy for discussions. This work was supported, in part, by the ANSEF, Grant No. 05-PS-eng-728-31.

- [1] S. Briauudeau, D. Bloch, and M. Ducloy, *Phys. Rev. A* **59**, 3723 (1999), and references therein.
- [2] D. Sarkisyan, D. Bloch, A. Papoyan, and M. Ducloy, *Opt. Commun.* **200**, 201 (2001).
- [3] G. Dutier, A. Yarovitski, S. Saltiel, A. Papoyan, D. Sarkisyan, D. Bloch, and M. Ducloy, *Europhys. Lett.* **63**, 35 (2003).
- [4] D. Sarkisyan *et al.*, *Phys. Rev. A* **69**, 065802 (2004).
- [5] D. Sarkisyan, T. Varzhapetyan, A. Papoyan, D. Bloch, M. Ducloy, in Proceedings of International Conference on Coherent and Nonlinear Optics (ICONO), St. Petersburg, Russia, 2005 (unpublished).
- [6] B. D. Agap'ev *et al.*, *Phys. Usp.* **36**, 763 (1993).
- [7] E. Arimondo, *Progress in Optics* (Elsevier Science, Amsterdam, 1996), Vol. 35, p. 257.
- [8] S. Harris, *Phys. Today* **50** (7), 36 (1997).
- [9] R. Wynands and A. Nagel, *Appl. Phys. B: Lasers Opt.* **68**, 1 (1999), and references therein.
- [10] M. D. Lukin *et al.*, *Phys. Rev. Lett.* **79**, 2959 (1997).
- [11] A. F. Huss *et al.*, *Phys. Rev. Lett.* **93**, 223601 (2004).
- [12] Z. D. Liu, P. Juncar, D. Bloch, and M. Ducloy, *Appl. Phys. Lett.* **69**, 2318 (1996).
- [13] P. Schwindt *et al.*, *Appl. Phys. Lett.* **85**, 6409 (2004).
- [14] S. Knappe, L. Hollberg, and J. Kitching, *Opt. Lett.* **29**, 388 (2004).
- [15] U. Rasbach *et al.*, *Phys. Rev. A* **70**, 033810 (2004).
- [16] J. Vanier, A. Godone, and F. Levi, *Phys. Rev. A* **58**, 2345 (1998).
- [17] D. Petrosyan and Yu. P. Malakyan, *Phys. Rev. A* **61**, 053820 (2000).
- [18] H. N. de Freitas, M. Oria, and M. Chevrollier, *Appl. Phys. B: Lasers Opt.* **75**, 703 (2002), and references therein.
- [19] G. Nikogosyan, D. Sarkisyan, and Yu. Malakyan, *J. Opt. Technol.* **71**, 602 (2004).
- [20] D. Budker, V. Yashchuk, and M. Zolotarev, *Phys. Rev. Lett.* **81**, 5788 (1998).
- [21] T. Varzhapetyan *et al.*, *Proc. SPIE* **5830**, 196 (2005).
- [22] B. Gross, N. Papageorgiou, V. Sautenkov, and A. Weis, *Phys. Rev. A* **55**, 2973 (1997).
- [23] B. Zambon and G. Nienhuis, *Opt. Commun.* **143**, 308 (1997).
- [24] A. Sargsyan, D. Sarkisyan, D. Staedter, and A. Akulshin, *Opt. Spectrosc.* (to be published).
- [25] A. Nagel, C. Affolderbach, S. Knappe, and R. Wynands, *Phys. Rev. A* **61**, 012504 (1999).
- [26] K. Motomura and M. Mitsunaga, *J. Opt. Soc. Am. B* **19**, 2456 (2002).
- [27] G. Dutier *et al.*, *Phys. Rev. A* **72**, 040501(R) (2005).
- [28] D. Sarkisyan *et al.*, Technical Digest of 2004 Conference on Lasers and Electro-Optics (CLEO/IQEC 2004), Report No. IMA1, San Francisco, 2004 (unpublished).
- [29] D. Sarkisyan, A. Papoyan, T. Varzhapetyan, K. Blush, and M. Auzinsh, *J. Opt. Soc. Am. B* **22**, 88 (2005).
- [30] I. Hamdi *et al.*, *Laser Phys.* **5**, 987 (2005), and references therein.